Available online www.jsaer.com

***Journal of Scientific and Engineering Research*, 2019, 6(2):100-109**

Research Article

ISSN: 2394-2630
CODEN(USA): JSERBR

Research of the Active Tectonic of Kilikya Region by Wavelet Analysis

Ali Muhittin ALBORA

Istanbul University-Cerrahpaşa Engineering Faculty, Geophysical Department, 34320 Avcılar, Istanbul, Turkey

Abstract In this study, wavelet analysis was applied to the geophysical data of the İskenderun region, which has a very complex structure in terms of tectonics, and tectonic elements belonging to the region were tried to be revealed. The region is located in the south of Turkey and is actively active in Africa, Anatolia and Arabic plates. The area where these three levans intersect, which is called Maras Joint, is located to the east of the Cilicia region and very young tectonic structures and discontinuities dominate the region due to the formation of the joint. The interaction of the plates is controlled by two major fault zones. But the continuity of these fault zones with each other is still a matter of debate.

Keywords Wavelet; Kilikya region; Magnetic anomaly map

Introduction

In geophysics, magnetic data occurs because of underground sources interacting with each other. The targets are small-sized objects at shallow depth. The success of numerical and approximation methods is determined by how well the target particles are separated. The wavelet transform decomposes the data into different components, and each component assigns a weight value. In terms of signal processing, the wavelet method defines a scale with a scale that varies depending on frequency and time. Thus, the wavelet method falls against the settling in time-frequency space. The wavelet method can be used for different resolutions and scales. This concept is called Multi-Resolution Analysis (MRA) analysis. Two- and three-dimensional filter studies can be performed using the wavelet method [1-6]. In this method, we can use various coefficients and the residual structure can be found as much as the desired number of repetitions. In this study, using Daubechies coefficients, step 1 can also achieve the desired results [7]. Another important feature of the study is the ability to obtain horizontal, vertical and diagonal outputs of the residual anomaly map that we want to obtain. We will then be able to interpret the different outputs obtained. İskenderun Gulf, which is a working region, is located at the point of interaction of Africa, Arab and Anatolian Plates, in the north-east of the Mediterranean. It has a very complex tectonic character with the interaction of Africa and Anatolian Plates in the West and the collisions of the Arab and Anatolian Plates in the east. During the Middle Miocene, the Arabic Plate was separated from the African Plate along the leftward Dead Sea Fay Zone (DSFZ). The Arabic Plate leaves the border of the Eurasian Plate along the Bitlis throne. After the escape tectonics that formed after the plate movements in this area, two important transform faults developed (North Anatolian Fault Zone and Eastern Anatolian Fault Zone (DAF)). As mentioned in the chapters above, DAF causes considerable debate about the later part of Marash's joint, which is regarded as the place where the three plates join. The most important cause of these discussions is that the fault cannot be tracked topographically and geologically. For this reason, geophysical data collected in the Iskenderun Basin (especially the intracorporeal data) may reveal us a little more about the subsequent orientation of DAF. For these reasons the region is regarded as an area where the most complex tectonism of your country is observed. [8-12] in order to illuminate the tectonics of the region in response to the geologic, geodetic and geological data. Many scientists who have used the solutions of large earthquakes in the region as seismological data have studied the characteristics of the faults dominating the region and the active tectonics of the region [12-15]. Determination of the structural boundaries as well as regional-residual separations from gravity and magnetic anomaly maps is also a very important problem. They developed a boundary technique to detect building boundaries [16]. They applied Wavelet technique to distinguish potential field anomalies [2] and [3]. Using the components of the wavelet method, they proved that the boundaries of the structure can be detected. They also applied the wavelet method to the archeojeophysical data and obtained very good results [4] and [17]. Fourier method and Wavelet method [18]. Theoretical studies on Wavelet [19-20]. In this study, a wavelet method was applied to the magnetic anomaly map of the Iskenderun Gulf [21]. They conducted studies on the earthquake activity and the formation of the Gulf of Osmaniye fault in the north-western part of Iskenderun Bay [22-24]. They investigated the tectonics of the Amanos Mountains, east of Iskenderun Bay [25-27].

Methods

The wavelet method was first used in 1909 in Haar's thesis. The most important feature of the Haar wavelet function is its tight support. However, the Haar wavelet function does not have a continuous basis. In the 1930's studies on variable-scale base functions, Littlewood, Paley, and Stein obtained functions that conserved energy at varying scales. In 1950-1960 Littlewood-Paley theory was applied to partial differential equations and integral equations. Between the years 1960-1980, Guido Weiss and Ronald Coifinan were able to recreate the space of functions by means of these atoms, working on the functions that atomic names describe as the simplest elements of a function space. Two and three dimensional filtering studies can be done using wavelet method [28, 29]. In this method, we can use various coefficients, we can find the residuals as many as the number of repetitions we want. In our work, we mostly get the results we want in Level 1 or 2, mostly using Daubechies coefficients. Another important feature of our work is that we can obtain Horizontal, Vertical and Diagonal outputs. Thus, we have the opportunity to interpret the different outputs obtained. Wavelet method can be expressed by Wavelet Transform and Multi-Resolution Analysis. According to this;

The class of functions that present the wavelet transform are those that are square integrals on the real time. This class is denoted as $L^2(R)$.

$$f(x) \in L^2(R) \Rightarrow \int_{-\infty}^{+\infty} |f(x)|^2 \, dx < \infty \tag{1}$$

The set of functions that are generated in the wavelet analysis are obtained by dilating (scaling) and translating (time shifting) a single prototype function, called the mother wavelet. The wavelet function $\psi(x) \in L^2(R)$ has two characteristic parameters, called dilation (a) and translation (b), which vary continuously. A set of wavelet basis function $\psi_{a,b}(x)$ may be given as [2],

$$\psi_{a,b}(x) = \frac{1}{\sqrt{|a|}} \psi\left(\frac{x-b}{a}\right) \qquad a, b \in R\,;\, a \neq 0 \tag{2}$$

Here, the translation parameter, "b", controls the position of the wavelet in time. The "narrow" wavelet can access high frequency information, while the more dilated wavelet can access low frequency information. This means that the parameter "a" varies for different frequencies. The continuous wavelet transform is defined by [2],

$$W_{a,b}(f) = \langle f, \psi_{a,b} \rangle = \int_{-\infty}^{+\infty} f(x)\, \psi_{a,b}(x)\, dx\,. \tag{3}$$

The wavelet coefficients are given as the inner product of the function being transformed with each basis function [2].

Daubechies (1990) invented one of the most elegant families of wavelets. They are called Compactly Supported Orthonormal Wavelets, and are used in Discrete Wavelet Transform (DWT). In this approach, the scaling function is used to compute the ψ. The scaling function $\phi(x)$ and the corresponding wavelet $\psi(x)$ are defined by [2],

$$\phi(x) = \sum_{k=0}^{N-1} c_k \, \phi(2x-k) \tag{4}$$

$$\psi(x) = \sum_{k=0}^{N-1} (-1)^k c_k \phi(2x+k-N+1) \tag{5}$$

where N is an even number of wavelet coefficients c_k, k= 0 to N-1. The discrete presentation of an orthonormal compactly supported wavelet basis of $L^2(R)$ is formed by dilation and translation of signal function $\psi(x)$, called the wavelet function. It is assumed that the dilation parameters "a" and "b" take only the discrete values: $a = a_0{}^j$, $b = k b_0 a_0{}^j$, where $k, j \in Z$, $a_0 > 1$, and $b_0 > 0$. The wavelet function may be rewritten as [2],

$$\psi_{j,k}(x) = a_0{}^{-j/2} \psi(a_0{}^{-j} x - k b_0) \tag{6}$$

and, the Discrete-Parameter Wavelet Transform (DPWT) is defined as:

$$\mathrm{DPWT}(f) = \langle f, \psi_{j,k} \rangle = \int_{-\infty}^{+\infty} f(x) a_0{}^{-j/2} \psi(a_0{}^{-j} x - k b_0) dx \tag{7}$$

The dilations' and translations' choise is chosen based on power of two, so called dyadic scales and positions, which make the analysis efficient and accurate. In this case, the frequency axis is partitioned into bands by using the power of two for the scale parameter "a". Considering samples at the dyadic values, one may get $b_0 = 1$ and $a_0 = 2$, and then the discrete wavelet transform becomes [2],

$$\mathrm{DPWT}(f) = \langle f, \psi_{j,k} \rangle = \int_{-\infty}^{+\infty} f(x) \{2^{-j/2} \psi(2^{-j} x - k)\} dx \ . \tag{8}$$

Here, $\psi_{j,k}(x)$ is defined as [2],

$$\psi_{j,k}(x) = 2^{-j/2} \psi(2^{-j} x - k), \qquad j,k \in Z \tag{9}$$

Mallat (1989) introduced an efficient algorithm to perform the DPWT known as the Multi-Resolution Analysis (MRA). It is well known in the signal processing area as the Two-Channel Sub-Band Coder. The MRA of $L^2(R)$ consists of successive approximations of the space V_j of $L^2(R)$. It does exist a scaling function $\phi(x) \in V_0$ such that [2].

$$\phi_{j,k}(x) = 2^{-j/2} \phi(2^{-j} x - k); \quad j,k \in Z \tag{10}$$

For the scaling function $\phi(x) \in V_0 \subset V_1$, there is a sequence $\{h_k\}$,

$$\phi(x) = 2 \sum_k h_k \, \phi(2x-k) \tag{11}$$

This equation is known as the two-scale difference equation. Furthermore, let us define W_j as a complementary space of V_j in V_{j+1}, such that $V_{j+1} = V_j \oplus W_j$ and $\bigoplus_{j=-\infty}^{+\infty} W_j = L^2(R)$. Since the $\psi(x)$ is a wavelet and it is also an element of V_0, a sequence $\{g_k\}$ exists such that [2],

$$\psi(x) = 2 \sum_k g_k \, \phi(2x-k) \tag{12}$$

It is concluded that the multiscale representation of a signal *f(x)* may be achieved in different scales of the frequency domain by means of an orthogonal family of functions $\phi(x)$. Now, let us see how the function in V_j is computed. The projection of the signal $f(x) \in V_0$ on V_j defined by $P_v f^i(x)$ is given by [2],

$$P_v f^i(x) = \sum_k c_{j,k}\,\phi_{j,k}(x) \tag{13}$$

Here, $c_{j,k} =< f, \phi_{j,k}(x) >$. Similarly, the projection of the function *f(x)* on the subspace W_j is also defined by [2],

$$P_w f^j(x) = \sum_k d_{j,k}\psi_{j,k}(x) \tag{14}$$

where $d_{j,k} =< f, \psi_{j,k}(x) >$. Because $V_j = V_{j-1} \oplus W_{j-1}$, the original function $f(x) \in V_0$ can be rewritten as [2],

$$f(x) = \sum_k c_{j,k}\,\phi_{j,k}(x) + \sum_j^{J-1}\sum_k d_{j,k}\,\psi_{j,k}(x) \qquad J > j_0 \tag{15}$$

The coefficients $c_{j,k}$ and $d_{j,k}$ are given by [2],

$$c_{j-1,k} = \sqrt{2}\sum_i h_{i-2k}\; c_{j,k} \tag{16}$$

and

$$d_{j,k} = \sqrt{2}\sum_j g_{j-2k}\; c_{j,k}\,. \tag{17}$$

The multiresolution representation is linked to Finite Impulse Response (FIR) filters. The scaling function ϕ and the wavelet ψ are obtained using the filter theory and consequently the coefficients are also defined by the last two equations. If at *x=t/2*, $F\{\phi(x)\}$ is considered and [2],

$$\Phi(\omega) = H\left(\frac{\omega}{2}\right)\Phi\left(\frac{\omega}{2}\right) \tag{18}$$

As $\phi(0) \neq 0$, *H*(0)=1, this means that *H*(ω) is a low-pass filter. According to this result $\phi(t)$ is computed by the low-pass filter *H*(ω). The mother wavelet $\psi(t)$ is computed by defining the function *G*(ω) so that $H(\omega)G^*(\omega) + H(\omega+\pi)G^*(\omega+\pi) = 0$. Here, *H*(ω) and *G*(ω) are quadrature mirror filters for MRA solution [2].

$$G(\omega) = -\exp(-j\omega)\,H^*(\omega+\pi) \tag{19}$$

Substituting *H*(0)=1 and *H*(π)=0, it yields *G*(0)=0 and *G*(π) =1, respectively. This means that *G*(ω) is a high pass filter. As a result, the MRA is a kind of Two-Channel Sub-Band Coder used in the high-pass and low-pass filters, from which the original signal can be reconstructed [2].

Since a major potential application of wavelets is in image processing, 2-D wavelet transform is a necessity. The subject, however, is still at an evolving stage and in this section only the extension of 1-D wavelets to the 2-D case will be discussed. The idea is first to form a 1-D sequence from the 2-D image row sequences, do a 1-D MRA, restore the MRA outputs to a 2-D format and repeat another MRA to the 1-D column sequences. The two steps of restoring to a 2-D sequence and forming a 1-D column sequence can be combined efficiently by appropriately selecting the proper points directly from the 1-D MRA outputs. After the 1–D row MRA, each low pass and high pass output goes through a 2-D restoration and 1-D column formation process and then move on to another MRA. Let x_1 and x_2 , be the 2-D coordinates and *H* = low-pass, *G*= high-pass. Then the 2-D separable scaling function is [2],

$$\phi^{(1)}(x_1, x_2) = \phi(x_1)\phi(x_2)\ , \quad HH \tag{20}$$

original signal can be reconstructed. Then 2-D separable wavelets are

$$\psi^{(2)}(x_1, x_2) = \phi(x_1)\psi(x_2)\ , \quad HG \tag{21}$$

$$\psi^{(3)}(x_1, x_2) = \psi(x_1)\phi(x_2) \quad , \quad GH \tag{22}$$

$$\psi^{(4)}(x_1, x_2) = \phi(x_1)\phi(x_2) \quad , \quad GG \tag{23}$$

with the corresponding wavelet coefficients [2].

The scheme of separable 2-D processing, while being simple and uses available 1-D filters, has disadvantages when compared to a genuine, 2-D MRA with non-separable filters. The latter is more freely designed and can provide a better frequency and even linear phase response, and has non-rectangular sampling [2], [20].

General Tectonics of the Study Area

Because the Study Area has a very complex structure, most researchers have defined it as a natural laboratory. The tectonics of the zone generally interact under the influence of the DAF and the Dead Sea Fault Zone (DSF). What is more important here is that three tectonic plates are united in this region. The position of this junction is still open to debate. Most researchers here have worked on the DAF's course in this area and have worked on the position of the intersection of these three levans. DAFZ starts from Karlıova in the north and extends to Kahramanmaraş in the southwest. DAFZ is a NE-SW trending, left-handed strike-slip fault zone. CAFZ in Karlıova and DSF approximately Turkoglu in Kahramanmaraş form triple joints here. The length between these two points is at least 400 km.

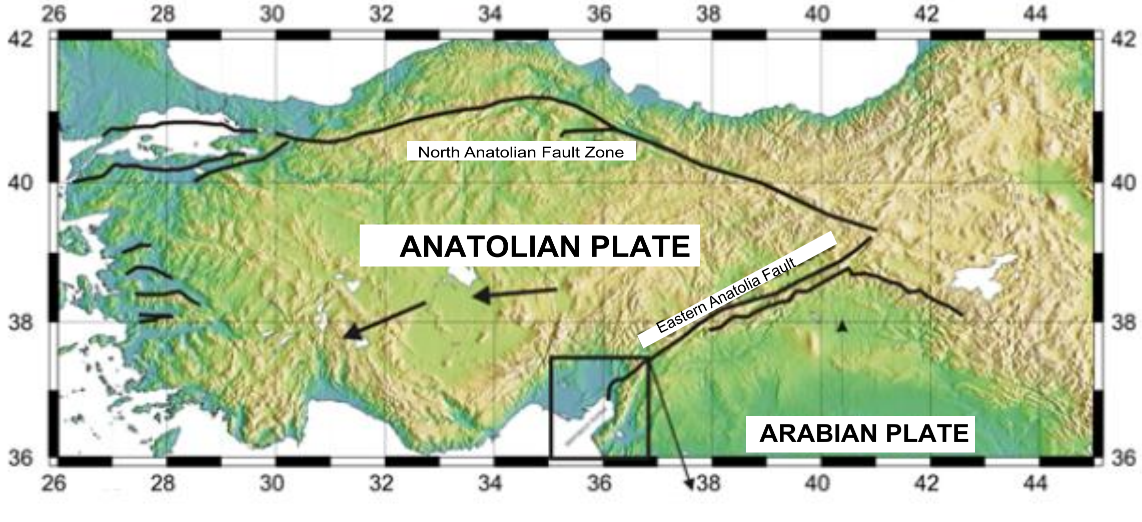

Figure 1: General Tectonics of the Eastern Mediterranean Region

The escape tectonics in Anatolia started in Pliocene. The eastern Anatolian Transform Fault with its left lateral strike and its associated structures separate the Iskenderun Basin and allow shallow delta deposits of the Plio-Quaternary Iskenderun Basin and its vicinity [21] and [22]. It can be said that the most important Neotectonic lineaments in the area that is very complicated in terms of tectonics are Amonos Fault, Karataş-Osmaniye Fault, Aslantaş Fault and DSF. Iskenderun The tectonic structure of the Gulf is distinguished as three different sediment units belonging to the Miocene and Quaternary periods (Fig. 2), [21]. Amanos mountains, east of Iskenderun Bay, Misis mountains and the units around them differ in lithological and tectonically. The formations that form the basis of the Amanos Mountains are Palaeozoic sandstone and green schists. These are Mesozoic limestone and ophiolite rocks. In the middle part of the Amanos Mountains, there are Palaeocene and Eocene limestone and middle Miocene aged shales and limestone. Middle Miocene shales and limestone are also discordant on Eocene strata. At the southern end of the mountainous region are marine Pliocene sediments. These formations which form the Amanos Mountains and the orographic extension tectonic directions and dislocation lines are similar.

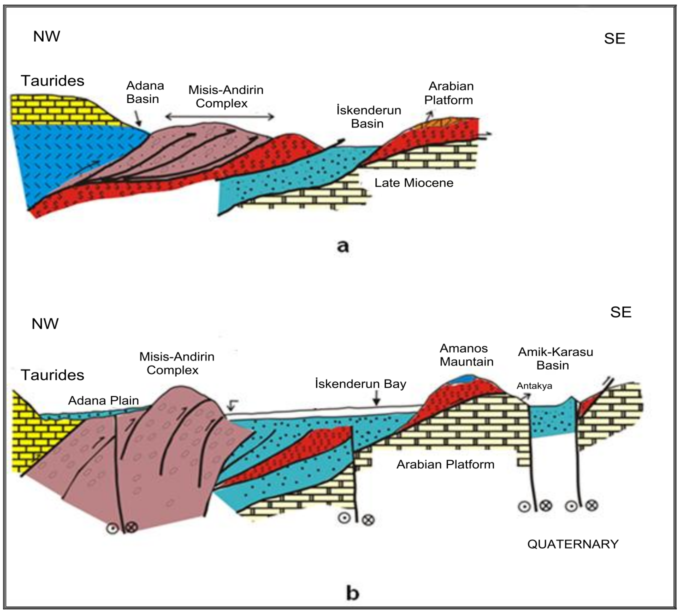

Figure 2: Evolution of the Iskenderun Basin (a) Late Miocene (b) Plio-Quaternary [21].

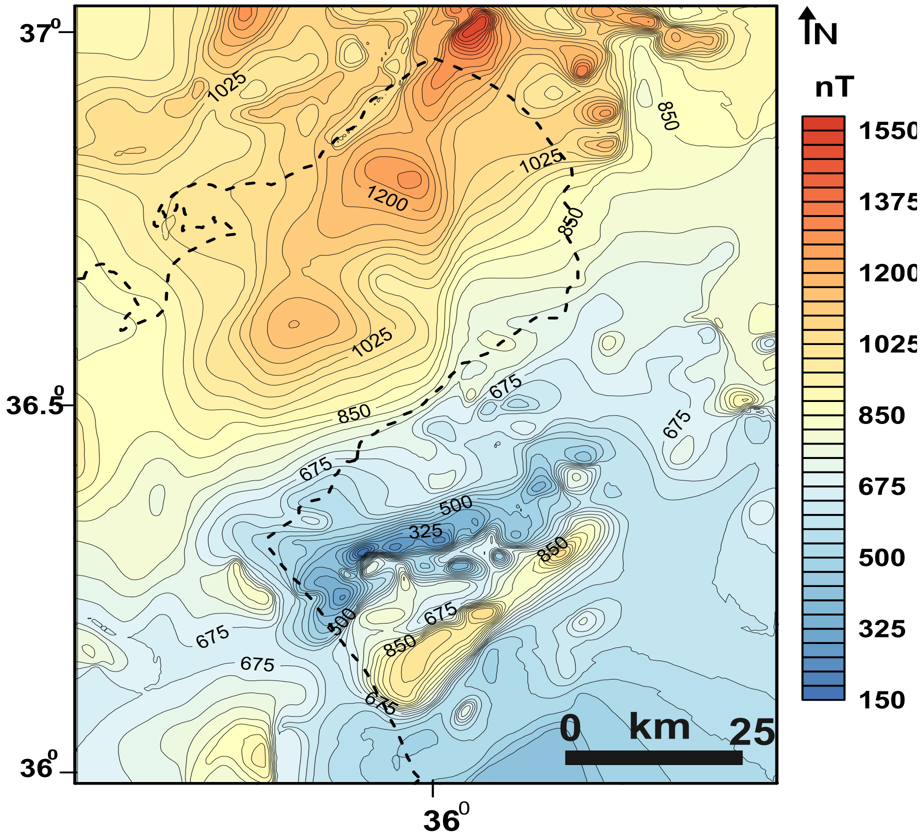

Figure 3: Magnetic anomaly map of Iskenderun Bay (Data obtained from Turkish Petroleum Corporation)

Evaluation of magnetic anomaly data

The magnetic anomaly map of the Iskenderun bay and its surroundings is given in Figure 3. In this map, although the Hatay region shows low values in the region where the Amanos Mountains are located, it shows 1500 nT in the gulf and in the northern part. As shown in Fig. 4, the regional structure is shown in Fig. 4a, which is horizontal in Fig. 4h1, vertical in Fig. 4v1 and cross components in Fig. 4d1.

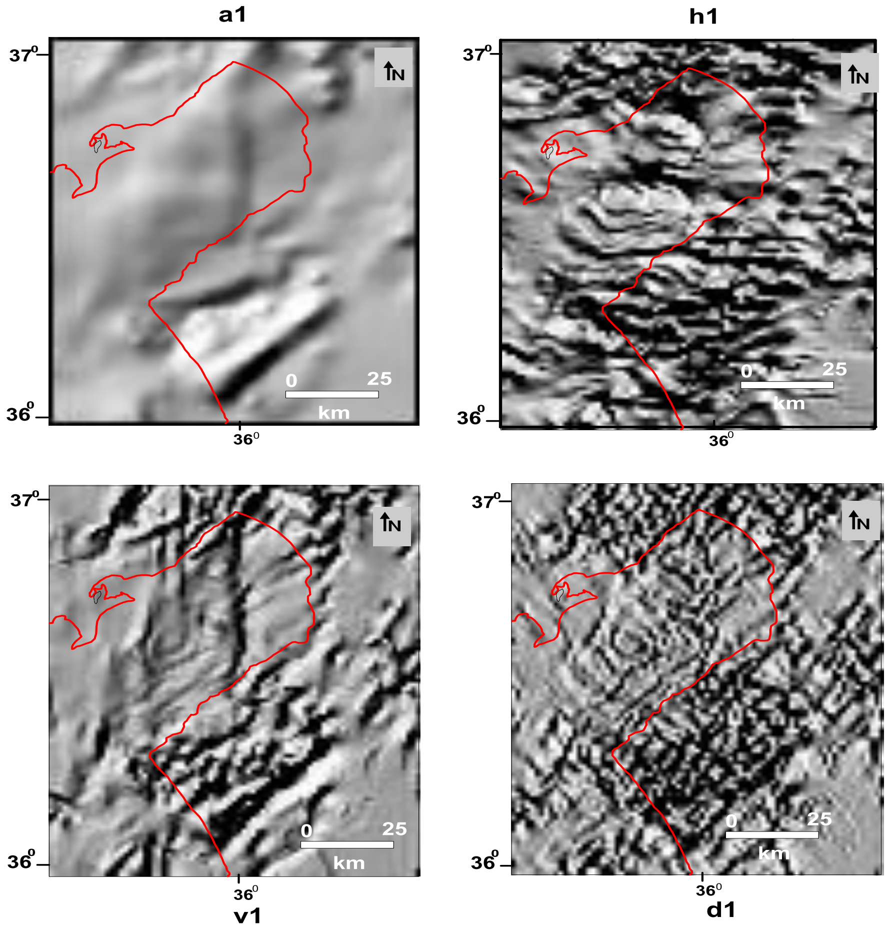

Figure 4: First order wavelet output of Iskenderun Bay aeronautical magnetic anomaly map (here: a, approximation, h, v, d detail coefficients).

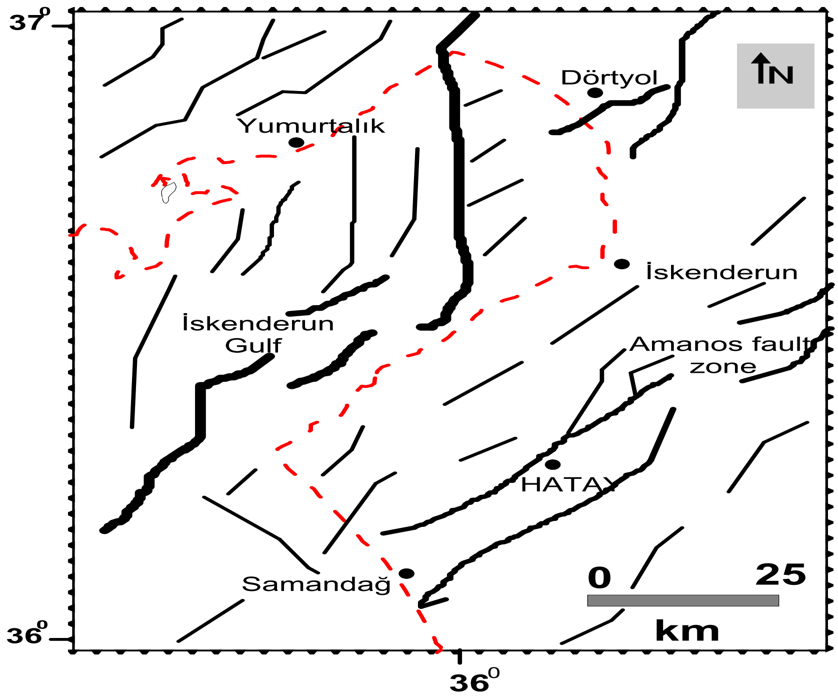

Figure 5: New tectonic map obtained from vertical component data after wavelet method applied to Iskenderun Bay magnetic anomaly map

Results and Discussion

Several studies have been conducted to determine the boundaries of geological structures in potential anomaly maps [30-36]. In this study, wavelet method was used to determine the boundaries of geological structures. Wavelet method has been used by many researchers in the determination of building boundaries [37-39]. Tectonic elements of Iskenderun bay and its surroundings were tried to be determined by using wavelet transform technique. The wavelet transform approach has been widely used in many disciplines today, and in recent years it has found a lot of usage in geophysical science. Wavelet transform is used to obtain the regional and residual anomaly maps of geophysical engineering, to determine the structure boundaries of potential source anomaly maps and to model these anomaly maps in recent times. Fourier transform, one of the data processing techniques applied to the wavelet method geophysical data, is successful because it removes some of its disadvantages. Figure 4 shows the results of applying the wavelet transform to the magnetic anomaly map given in Fig. It is seen here that the regional coefficients of the regional anomalies are very successful. When the detail coefficients of the wavelet transform are examined, we can say that the vertical, horizontal and diagonal components of the residual effect are clearly revealed in the first iteration and the boundaries of the structure are observed very clearly. From these results, a new tectonic map is obtained and the new tectonic map obtained in Fig. 5 is given. Another important point, which is the result of the vertical first level output of the magnetic data, is the large main fault zones (Karataş-Osmaniye and Amanos Faults) extending in the Gulf-limiting Gulf. These deformation zones, which are extensions of DAF, control the boundary between the ophiolite and other units in the gulf-confined areas. It is possible to see this clearly in geological, morphological, earthquake focal mechanism solutions and wavelet outputs obtained from magnetic data (For detailed information about the earthquake focus mechanisms, see [21]). He made a map of the depths by using the magnetic anomaly map of the Gulf of Iskenderun [40]. In this study, the fault system, which is named as İskenderun fault zone, beat the ophiolite base towards the Amanos Mountains and beat the formation of the gulf [40]. It is quite difficult to talk about a strike-slip tectonic that controls the ophiolite and other units within the Gulf, which is outside the predominant control of these two deformation zones. As a result of evaluation of seismic and magnetic data in the İskenderun bay, the presence of a structure extending in the direction of the KG was determined in the bay. While this structure has lost its ascension in the northern parts of the bay, it still shows an expansion in these regions. The K-G trending flower constructions, which cut young sediments and clearly observed, are not compatible with the dominant NE-GB tectonic direction in the region. Two reasons can be put forward for this reason. First view, these faults developed as a KG-oriented grabenin patcher that existed before the formation of DAF and behaved as normal faults, but nowadays they are working as strike-slip faults under the influence of DAF. The second view is that the DAF has degenerated by raising or lowering the Iskenderun Gulf between the Karataş-Osmaniye Fault and the Amonos Fault. This deformation gave rise to deformation zones (K-G) running in contrast to the direction of dominant tectonic elements (NE-GB).

References

[1]. Fedi, M., & Quata, T (1998). Wavelet Analysis for the regional-residual and local separation at potential field anomalies. *Geophys. Prospect.*, (46): 507-525.

[2]. Uçan, ON., Şeker, S., Albora, AM., & Özmen, A (2000). Separation of Magnetic Field Data Using 2-D Wavelet approach. *Journal of The Balkan Geophysical Society*, (3): 53-58.

[3]. Uçan, ON., Albora, AM., & Hisarlı, ZM (2001). Comments on the Gravity and Magnetic Anomalies of Saros Bay using Wavelet approach. *Marine Geophysical Researches*, (22): 251-264.

[4]. Albora, AM., Hisarlı, ZM., & Uçan, ON (2004). Application of Wavelet Transform to Magnetic Data Due to Ruins of Hittite Civilization in Turkey. *Pure and Applied Geophysics*, (161): 907-930.

[5]. Albora, AM., Bal, A., & Uçan, ON (2007). A new approach for border detection of Dumluca (Turkey) iron ore area: Wavelet Cellular Neural Networks. *Pure and Applied Geophysics*, (164): 119-215.

[6]. Alp H., Albora AM., & Tur H (2011). A View of Tectonic Structure and Gravity Anomalies of Hatay Region Southern Turkey Using Wavelet Analysis. *Journal of Applied Geophysics*, (75): 498-505.

[7]. Daubechies, I (1990). The Wavelet Transform, Time-Frequency Localization and Signal Analysis. *IEEE Trans, On Information Theory*, 36.

[8]. Mc Kenzie, DP (1972). Active tectonics of the Mediterranean Region. *Geophs. J. R. Astron. Soc*., (30): 109-185.

[9]. Nur, A., & Ben-Avraham, Z (1978). The Eastern Mediterranean and the Levant: Tectonics of Continental Collision. *Tectonophysics*, (46): 279-311.

[10]. Erdoğan, D., Uçan, ON., Albora, AM., & Özmen, A (2005). Application of the Steerable Filters for gravity anomaly map of Hatay region, *Fourth International Conference on Electrical and Electronics Engineering*, Turkey-Bursa, 185.

[11]. Alp H., & Albora, AM (2008). A look at the lineals in the Eastern Anatolian Fault using the wavelet analysis method. *16. Signal Processing and Communication Applications Convention*, 20-22 April Didim-Aydın Turkey, 262.

[12]. Alp, H., Tur, H. & Albora, AM (2011). Investigation of The Tectonic Structure of Cilicia Basin by Applying Wavelet Analysis Method To Gravity Data. *EGU Geophysical Research Abstracts*, 13, 208.

[13]. Mc Kenzie, DP (1972). Active tectonics of the Mediterranean Region. *Geophs. J. R. Astron. Soc.*, (30): 109-185.

[14]. Le Pichon, X. & Angelier, J (1979). The Hellenic arc and trench system: a key to the Neotectonic evolution of The Eastern Mediterranean Area. *Tectonohypsics,* (117): 259-294.

[15]. Taymaz, T., Eyidoğan H., & Jackson J (1991). Source parameters of large earthquakes in the East Anatolian Fault Zone (Turkey). *Geophys. J. Int.*, (106): 537-550.

[16]. Fedi M. & Florio. G (2001). Detection of potential fields source boundaries by enhanced horizontal derivative method. *Geophysical Prospecting* (49): 40-58.

[17]. Albora, AM., Uçan, ON., Hisarlı, ZM. & Stümpel, H (2002). Archaeogeophysical Investigation of Sivas-Belted Hittite Civilization Using Wavelet Method. *Uygulamalı Yerbilimleri-Kocaeli Üniversitesi*, (1): 125-134.

[18]. Alp, H., Akıncı, TÇ., & Albora, AM (2008). Comparison of Fourier and Wavelet Transformations in Geophysical Applications. *Journal of Engineering Sciences*, 14 (1): 67-76.

[19]. Albora, AM & Uçan, ON (2001). Gravity Anomaly Separation Using 2-D Wavelet Approach and average depth calculate. *Doğuş Dergisi-Doğuş Üniversitesi*, (3): 1-13.

[20]. Chan Y.T., 1996, Wavelet Basics, Kluwer Academic Publishers, USA.

[21]. Albora, AM., Sayın, N., & Ucan, ON (2006). Evaluation of Tectonic Structure of İskenderun Basin (Turkey) Using Steerable Filters. *Marine Geophysical Researches,* (27): 225-239.

[22]. Aksu, AE., Calon, TJ., Hall, J., & Yasar, D (2005). Origin and evolution of the Neogene Iskenderun Basin, northeaster Mediterranean Sea. *Mar. Geol*., (221): 161-187.

[23]. Güçtekin, A. (2018). Petrogenesis of plio-quaternary intra-plate continental alkaline lavas from İskenderun the Gulf (Southern Turkey): Evidence for metasomatized lithospheric mantle. *Chemie der Erde.*, 1-14.

[24]. Oyan, V. (2018). Petrogenesis of the Quaternary mafic alkaline volcanism along the African-Anatolian plates boundary in Turunçlu-Delihalil (Osmaniye) region in southern Turkey. *Lithos,* (314): 630-645.

[25]. Öztürk, M.Z., Şener, M.F., Şener, M. & Şimşek, M. (2018). Structural controls on distribution of dolines on Mount Anamas (Taurus Mountains, Turkey). *Geomorphology*, (317): 107-116.

[26]. Over S., Akın, U. & Şen, R. (2018). Geophysical Data (Gravity and Magnetic) from the Area between Adana, Kahramanmaraş and Hatay in the Eastern Mediterranean Region: Tectonic Implications. *Pure and Applied Geophysics*, (175): 2205-2219.

[27]. Özdemir, A. & Şahinoğlu, A. (2018). Prospective Areas For Petroleum Exploration and Oil & Gas Potential of the onshore Hatay (Southern Turkey). *Section Oil and Gas Exploration, 18th International Multidisciplinary Scientific GeoConference SGEM 2018.* 719-726.

[28]. Xu, C., Wang, H., Luo, Z. Liu, H. & Liu, X. (2017). Insight into Urban Faults by Wavelet Multi-Scale Analysis and Modeling of Gravity Data in Shenzhen, China. *Journal of Earth Science*, (20): 1-9.

[29]. Lawal, T. O., Nwankwo, L.I. & Akoshile, C.O. (2015). Wavelet Analysis of Aeromagnetic Data of Chad Basin, Nigeria. *The African Review of Physics*, (10): 111-120.

[30]. Eshaghzadeh, A., Dehghanpour, A. & Kalantari, R.A. (2018). Application of the tilt angle of the balanced total horizontal derivative fi lter for the interpretation of potential field data. (59). 161-178.

[31]. Pham, L.T., Oksum, E., Do, T.D. and Huy, M.L. (2018). M. L. New method for edges detection of magnetic sources using logistic function. DOI: 10.24028/gzh.0203-3100.v40i6.2018.151033.

[32]. Albora, A.M. (2018). Interpretation of the gravity anomaly map of the Sivas (Dumluca) - Turkey iron ore using the Cellular Neural Network (CNN) method. *Journal of Scientific and Engineering Research*, (7): 283-292.

[33]. Görgün, E. and Albora, A. M (2017). Seismotectonic Investigation of Biga Peninsula in SW Marmara Region Using Steerable Filter Technique, Potential Field Data and Recent Seismicity. Pure and Applied Geophysics, (174): 3889-3904.

[34]. Albora, A.M. (2017). Investigation of Tectonic Structure of Turkey-Hatay Region Using Markov Random Fields (MRF). (5): 86-93.

[35]. Uçan, O.N. Bilgili, E. and Albora, A.M. (2002). Magnetic Anomaly Separation Usıng Genetic Cellular Neural Networks. *Journal of the Balkan Geophysical Society*. (5): 65-70.

[36]. Bilgili, E., Göknar, C., Albora, A.M. and Uçan, O.N. (2005). Potential Anomaly Separation and Archeological Site Localization Using Genetically Trained Multi-level Cellular Neural Networks. (27): 294-303.

[37]. Albora, A.M. (2018). Detection of Building Boundaries in Mine Fields using Wavelet Method. *Journal of Scientific and Engineering Research*, (3): 407-414.

[38]. Albora, A.M. and Uçan, O.N. (2001). Gravity anomaly separation using 2-D wavelet approach and average depth calculation. *Doğuş Üniversitesi Dergisi* (1): 1-12.

[39]. Oruç, B. (2014). Structural interpretation of south part of western anatolian using analytic signal of the second order gravity gradients and discrete wavelet transform analysis. Journal of Applied Geophsics, 103, 82-98.

[40]. Demirel, S.A. (1995). Interpretation of Magnetic data of Iskenderun Gulf, Journal of Geophysics, (9): 45-50.